From balance to imbalance: a shift in the dynamic behaviour of Chhota Shigri glacier, western Himalaya, India

Mohd Farooq AZAM,[1] Patrick WAGNON,[2] Alagappan RAMANATHAN,[1] Christian VINCENT,[3] Parmanand SHARMA,[1] Yves ARNAUD,[2] Anurag LINDA,[1] Jose George POTTAKKAL,[1] Pierre CHEVALLIER,[4] Virendra Bahadur SINGH,[1] Etienne BERTHIER[5]

[1]*School of Environmental Sciences, Jawaharlal Nehru University, New Delhi 110067, India*
[2]*IRD/UJF – Grenoble I/CNRS/G-INP, LGGE UMR 5183, LTHE UMR 5564, 38402 Grenoble Cedex, France*
E-mail: patrick@lgge.obs.ujf-grenoble.fr
[3]*UJF – Grenoble I/CNRS, LGGE UMR 5183, 38041 Grenoble Cedex, France*
[4]*Laboratoire Hydrosciences (UMR 5569 – CNRS, IRD, Montpellier Universities 1 and 2), Université Montpellier 2, 34095 Montpellier Cedex 5, France*
[5]*Legos, CNRS, Université de Toulouse, 31400 Toulouse Cedex, France*

ABSTRACT. Mass-balance and dynamic behaviour of Chhota Shigri glacier, western Himalaya, India, has been investigated between 2002 and 2010 and compared to data collected in 1987–89. During the period 2002–10, the glacier experienced a negative glacier-wide mass balance of -0.67 ± 0.40 m w.e. a^{-1}. Between 2003 and 2010, elevation and ice-flow velocities slowly decreased in the ablation area, leading to a 24–37% reduction in ice fluxes, an expected response of the glacier dynamics to its recent negative mass balances. The reduced ice fluxes are still far larger than the balance fluxes calculated from the 2002–10 average surface mass balances. Therefore, further slowdown, thinning and terminus retreat of Chhota Shigri glacier are expected over the next few years. Conversely, the 2003/04 ice fluxes are in good agreement with ice fluxes calculated assuming that the glacier-wide mass balance is zero. Given the limited velocity change between 1987–89 and 2003/04 and the small terminus change between 1988 and 2010, we suggest that the glacier has experienced a period of near-zero or slightly positive mass balance in the 1990s, before shifting to a strong imbalance in the 21st century. This result challenges the generally accepted idea that glaciers in the Western Himalaya have been shrinking rapidly for the last few decades.

1. INTRODUCTION

Although Himalayan glaciers have important social and economic impacts (Barnett and others, 2005), they have not been monitored on a long-term basis and little is known about recent glacier trends or their contribution to local and regional water supplies. Because of this poor knowledge, the controversial statement that 'the likelihood of them disappearing by the year 2035 or perhaps sooner is very high if the Earth keeps warming at the current rate' came into existence in the Intergovernmental Panel on Climate Change (IPCC) Fourth Assessment Report (Solomon and others, 2007; Cogley and others, 2010). A generally negative mass balance of mountain glaciers on a global level is clearly revealed by recent research (Cogley, 2009; Zemp and others, 2009), but the effect of global warming in the Himalaya is still under debate (Yadav and others, 2004; Roy and Balling, 2005). Though temperate glacial mass-balance change is one of the best indicators of climate change (Oerlemans, 2001; Vincent and others, 2004; Ohmura and others, 2007), the paucity of mass-balance data in the Himalaya makes it difficult to obtain a coherent picture of regional climate-change impacts in this region. In the Indian Himalaya the first mass-balance study started on Gara Glacier, Himachal Pradesh, in September 1974 (Raina and others, 1977) and ended in 1983 (Dobhal and others, 2008). According to Dyurgerov and Meier (2005), eight glaciers in the Indian Himalaya were surveyed for mass balance for at least 1 year during the 1980s. Unfortunately each study was restricted to short periods, not more than one decade (Dobhal and others, 2008). Remote-sensing studies were also attempted in this part of the Himalaya, but these either deal with only surface area changes (e.g. Kulkarni and others, 2007; Bhambri and others, 2011) or cover short periods (Kulkarni, 1992; Berthier and others, 2007).

The present study is based on mass-balance and surface ice flow velocity measurements conducted on Chhota Shigri glacier, Himachal Pradesh, between 2002 and 2010, and on a comparison with data collected in 1987–89. In the Indian Himalaya, this is one of the longest continuous field mass-balance datasets. In October 2009, a ground-penetrating radar (GPR) survey was also conducted to measure ice thickness. Eight years of mass-balance measurements, surface ice velocities and ice thickness data provide an opportunity to study the behaviour of this glacier. The main objectives of this paper are (1) to present the recent mass balance of Chhota Shigri glacier, (2) to determine the ice fluxes at five cross sections from thickness and ice velocities and (3) to compare these data with the ice fluxes inferred from cumulative surface mass balance upstream of the same cross sections. These results give insights into the mass-balance trend of the glacier over the last two to three decades, and allow us to assess whether it is in equilibrium with the climate of the 21st century.

https://doi.org/10.3189/2012JoG11J123 Published online by Cambridge University Press

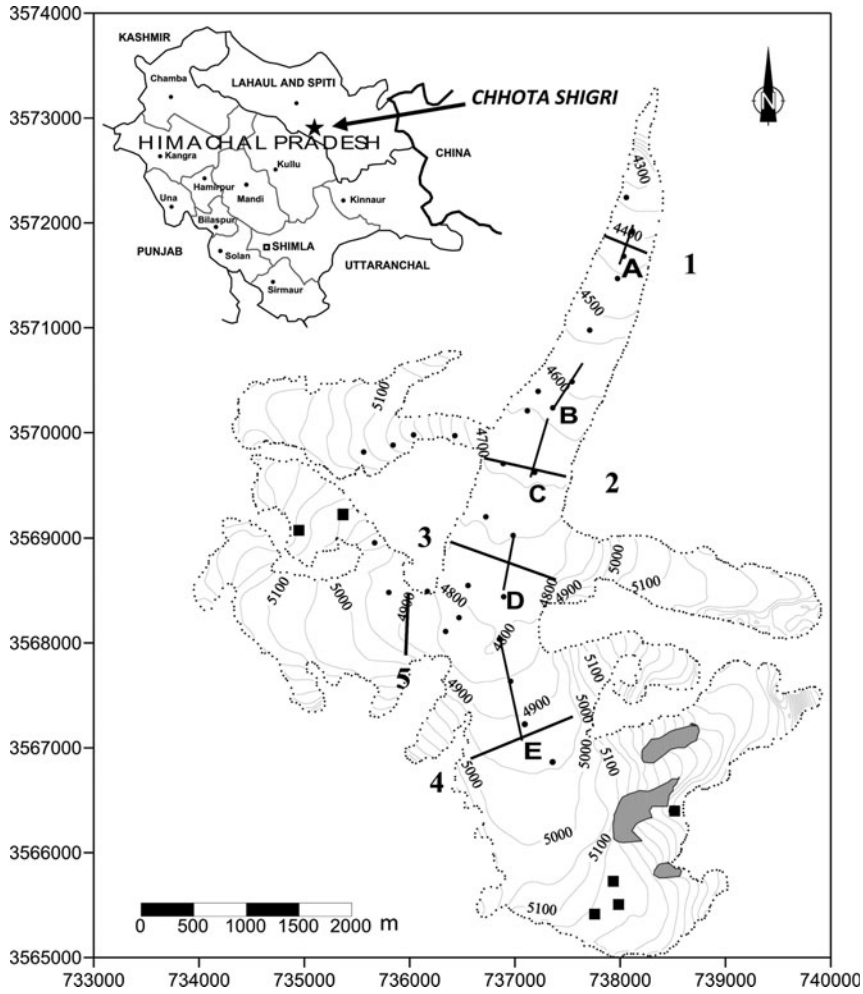

Fig. 1. Map of Chhota Shigri glacier with the measured transverse cross sections (lines 1–5), the ablation stakes (dots) and the accumulation sites (squares). Also shown are longitudinal sections (lines A–E) used to calculate thickness and ice velocity variations (see Section 4.2). The map (contour lines, glacier delineation) was constructed using two stereoscopic pairs of SPOT5 (Système Probatoire pour l'Observation de la Terre) images acquired on 12 and 13 November 2004 and 20 and 21 September 2005 (Wagnon and others, 2007). The map coordinates are in the UTM43 (north) World Geodetic System 1984 (WGS84) reference system.

2. SITE DESCRIPTION AND METHODOLOGY

2.1. Site description

Chhota Shigri glacier (32.2° N, 77.5° E) is a valley-type glacier located in the Chandra-Bhaga river basin of Lahaul and Spiti valley, Pir Panjal range, western Himalaya. This glacier extends from 6263 to ~4050 m a.s.l., is ~9 km long and covers an area of 15.7 km^2. Its snout is easy to locate from one year to the next because it is well defined, lying in a narrow valley and giving birth to a single proglacial stream. The main orientation of the glacier is north, but its tributaries have a variety of orientations (Fig. 1). The lower ablation area (<4400 m a.s.l.) is partly covered by debris representing ~3.4% of the total surface area. The glacier is located in the monsoon–arid transition zone and is influenced by two atmospheric circulation systems: the Indian monsoon during summer (July–September) and the Northern Hemisphere mid-latitude westerlies during winter (January–April) (Singh and others, 1997; Bookhagen and Burbank, 2006; Gardelle and others, 2011).

2.2. Mass balance

The first series of mass-balance measurements on Chhota Shigri glacier was performed between 1987 and 1989 (Nijampurkar and Rao, 1992; Dobhal and others, 1995; Kumar, 1999). The bedrock topography and surface ice velocity were also surveyed over the same period by gravimetric and stake displacement methods respectively (Dobhal and others, 1995; Kumar, 1999). We reinitiated the mass-balance observations in 2002. Since that year, annual surface mass-balance measurements have been carried out continuously on Chhota Shigri glacier at the end of September or the beginning of October using the direct glaciological method (Paterson, 1994). Ablation was measured through a network of ~22 stakes distributed between 4300 and 5000 m a.s.l. (Fig. 1), whereas in the accumulation area the net annual accumulation was obtained at six sites (by drilling cores or pits) between 5100 and 5550 m a.s.l. (Wagnon and others, 2007). In the accumulation area, the number of sampled sites is limited due to difficulty of access and the high elevation. The glacier-wide mass balance B_a is calculated according to

$$B_a = \sum b_i(s_i/S) \quad (1)$$

where b_i is the mass balance of the altitudinal range i (m w.e. a^{-1}), of map area s_i, and S is the total glacier area. For each altitudinal range, b_i is obtained from the corresponding stake readings or net accumulation measurements.

https://doi.org/10.3189/2012JoG11J123 Published online by Cambridge University Press

2.3. Surface velocity

Annual surface ice velocities were measured at the end of each ablation season (September–October) by determining the annual stake displacements (~22 stakes) using a differential GPS (DGPS). These geodetic measurements were performed in kinematic mode relative to two fixed reference points outside of the glacier on firm rocks. The accuracy of x (easting), y (northing) and z (elevation) at each stake position is estimated at ±0.2 m depending mainly on the size of the hole in which the stake was set up. Thus the surface ice velocities measured from stake displacements have an accuracy of ±0.3 m a^{-1}.

2.4. Ice thickness

GPR measurements were conducted in October 2009 to determine ice thickness on five transverse cross sections (Fig. 1) between 4400 and 4900 m a.s.l. A pulse radar system (Icefield Instruments, Canada) based on the Narod transmitter (Narod and Clarke, 1994) with separate transmitter and receiver, was used in this study with a frequency centred near 4.2 MHz and an antenna length of 10 m. Transmitter and receiver were towed in snow sledges along the transverse profile, separated by a fixed distance of 20 m, and used to record measurements every 10 m. The positions of the receiver and the transmitter are known through DGPS measurements, within an accuracy of ±0.1 m. The speed of electromagnetic wave propagation in ice has been assumed to be 167 m μs^{-1} (Hubbard and Glasser, 2005). The field measurements were performed in such a way as to obtain reflections from the glacier bed located more or less in the vertical plane with the measurement points at the glacier surface, allowing the glacier bed to be determined in two dimensions. The bedrock surface was constructed as an envelope of all ellipse functions, which give all the possible reflection positions between sending and receiving antennas. Ice thickness was measured along four transverse profiles (profiles 1–4) on the main glacier trunk and one (profile 5) on a western tributary (Fig. 1).

3. DATA ANALYSIS AND RESULTS

3.1. Glacier-wide mass balance and mass-balance profile

The annual glacier-wide mass balance and cumulative mass balance of Chhota Shigri glacier between 2002 and 2010 are plotted in Figure 2. The glacier-wide mass balance was negative except for three years (2004/05, 2008/09 and 2009/10). It varies from a minimum value of –1.42 m w.e. in 2002/03 to a maximum of +0.33 m w.e. in 2009/10. The cumulative mass balance of Chhota Shigri is –5.37 m w.e. between 2002 and 2010, while the glacier-wide mass balance averaged over the same period is –0.67 m w.e. a^{-1}.

The quantitative uncertainty associated with the glaciological mass balance requires a distinction between the accumulation zone and the ablation zone. In the accumulation zone, the surface mass-balance measurements were obtained from shallow boreholes (auger). Therefore, they are based on core length and density determination. In the ablation zone, the measurements have been carried out from ablation stakes. The overall errors (standard deviation) on point measurements are estimated at 0.30 and 0.15 m w.e. in the accumulation and ablation zones, respectively. The overall error comes from a variance analysis (Thibert and others, 2008) applied to all types of errors (ice/snow density, core length, stake height determination, liquid-water content of the snow, snow height). Although conducted on a glacier in the European Alps, the analysis of Thibert and others (2008) can be generalized to other glaciers because it is based on measurement errors that are similar on every glacier when using the glaciological method. However, only six sites are sampled in the accumulation zone (11.6 km^2), and 22 sites in the ablation zone (4.1 km^2). The uncaptured spatial variability of surface mass balance may cause systematic errors in the glacier-wide mass balance. In the accumulation zone, the spatial variability remains unknown and is probably very high as observed for other glaciers (e.g. Machguth and others, 2006). In the ablation zone, stakes set up at the same altitude show similar values except on the terminal tongue which is debris-covered (0.54 km^2). Consequently, the overall uncertainties in mass-balance profile have been assessed at 0.5 m w.e. in the accumulation zone, 0.25 m w.e. in the white ablation zone and 0.5 m w.e. in the debris-covered area of the glacier. The surface area estimation also causes systematic error. The estimated uncertainty in the surface area calculated for each altitudinal range is 5%. Combining these errors at different altitudinal ranges using Eqn (1), the uncertainty in the annual glacier-wide mass balance is 0.4 m w.e. a^{-1}. As revealed by other studies (e.g. Vincent, 2002; Thibert and others, 2008; Huss and others, 2009), this estimation confirms that the glaciological method needs to be calibrated by a volumetric method over a long period of monitoring (>5 years) in order to limit the systematic errors and improve the accuracy of absolute values of mass balance. Note that the uncertainty of relative changes in mass balance from year to year is smaller than those inherent in annual mass balances, as the influence of systematic errors can be reduced.

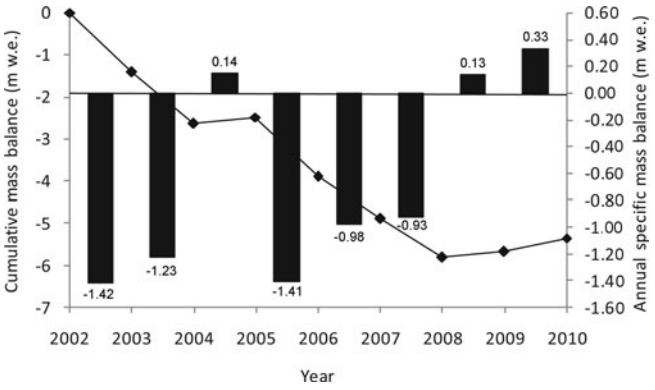

Fig. 2. Cumulative (line) and annual glacier-wide mass balances (histograms) of Chhota Shigri glacier during 2002–10. The value of annual glacier-wide mass balance (m w.e.) is also given with the corresponding histogram

We also calculated the mass-balance profile between 2002 and 2010 (Fig. 3). For each altitudinal range, we computed the average of all available measurements. Figure 3 shows that melting in the lowest part of the ablation area (<4400 m a.s.l.) is reduced by ~1 m w.e. a^{-1} irrespective of its altitude. This is due to the debris cover (approximately 5–10 cm thick debris mixed with isolated rocks) which reduces the melting in this region (Mattson and others, 1993; Wagnon and others, 2007). Moreover the lower part of Chhota Shigri glacier flows in a north–south-oriented deep and narrow valley (Fig. 1), causing the glacier

https://doi.org/10.3189/2012JoG11J123 Published online by Cambridge University Press

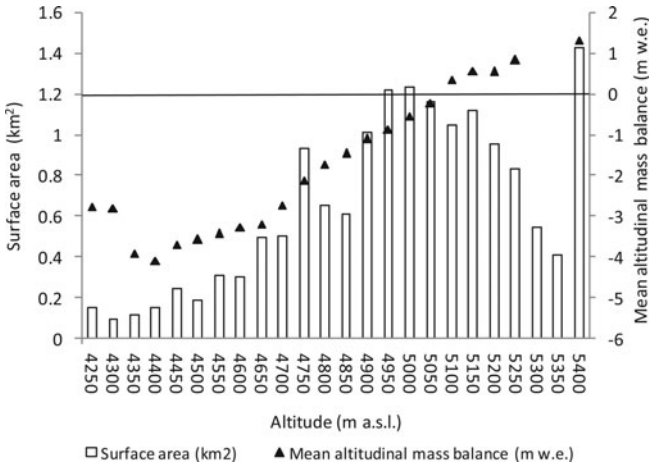

Fig. 3. The 2002–10 average mass-balance profile and hypsometry of Chhota Shigri glacier. Altitudinal ranges are of 50 m (e.g. 4400 stands for the range 4400–4450 m), except for 4250 and 5400 which stand for 4050–4300 and 5400–6250 m respectively.

tongue to receive less solar radiation due to the shading effect of the steep valley slopes.

3.2. Ice thicknesses and cross-sectional areas

Thanks to clear reflections, the ice/bedrock interface was generally easy to determine in all profiles. Figure 4 provides an example of the radargram obtained at cross section 2. A radar wave velocity of 167 m μs^{-1} was used to calculate ice thickness at all the profiles. The cross sections obtained from GPR measurements reveal a valley shape with maximum ice thickness greater than 250 m (Fig. 5). The centre-line ice thickness increases from 124 m at 4400 m a.s.l. (cross section 1 in Fig. 1) to 270 m at 4900 m a.s.l. (cross section 4). This confirms that the thicknesses obtained by gravimetric methods in 1989 (Dobhal and others, 1995), twice as low as the present results, were underestimated as proposed by Wagnon and others (2007). The cross-sectional areas are given in Table 1. The accuracy of the calculated ice thickness is determined, in part, by the accuracy of the measurement of the time delays and the antenna spacing. Additional errors may arise because the smooth envelope of the reflection ellipses is only a minimal profile for a deep valley-shape bed topography, with the result that the ellipse equation will be governed by arrivals from reflectors located toward the side and thus not directly beneath the points of observation. Further errors may be introduced by assuming that all reflection points lie in the plane of the profile rather than on an ellipsoid. No errors associated with radar wave velocity variations between snow and ice have been accounted for because all cross sections were surveyed in the ablation zone or slightly above (with the firn/ice transition depth at the surface or <2 m deep). Hence, the radar wave velocity for ice (167 m μs^{-1}) was used to calculate all ice depths. The estimated overall uncertainty in ice thickness is ±15 m. Given that the uncertainty in ice surface coordinates is low (±0.1 m), the uncertainty in cross-sectional areas mainly arises from the uncertainty in ice thickness. The uncertainties in cross-sectional areas are 16%, 9%, 10%, 10% and 15% for cross sections 1, 2, 3, 4 and 5 respectively.

3.3. Ice velocity

Annual surface ice velocities were also measured between 2002 and 2010. However, some data gaps exist due to discontinuous DGPS signal, or loss of stakes. The 2003/04 ice velocities were used in this study because they provided the most complete dataset (Fig. 6). The centre-line horizontal ice velocities at each cross section were calculated by linear interpolation along the centre line between the velocities measured immediately up- and downstream of the cross section (ablation stakes visible in Fig. 1). Mean cross-sectional velocities are required to compute the ice fluxes (see Section 3.4). A map of the surface ice velocity field was derived by correlating SPOT5 images acquired on 13 November 2004 and 21 September 2005 (Berthier and others, 2005). Comparison of the satellite-derived velocities with 16 nearly simultaneous DGPS velocity measurements shows a mean difference of 0.2 m a^{-1} and a standard deviation of 1.6 m a^{-1}. The ratio between the centre-line horizontal velocity and the mean surface velocity (all extracted from the satellite-derived 2004/05 velocity field) was found to be 0.80 and 0.78 for cross sections 2 and 3

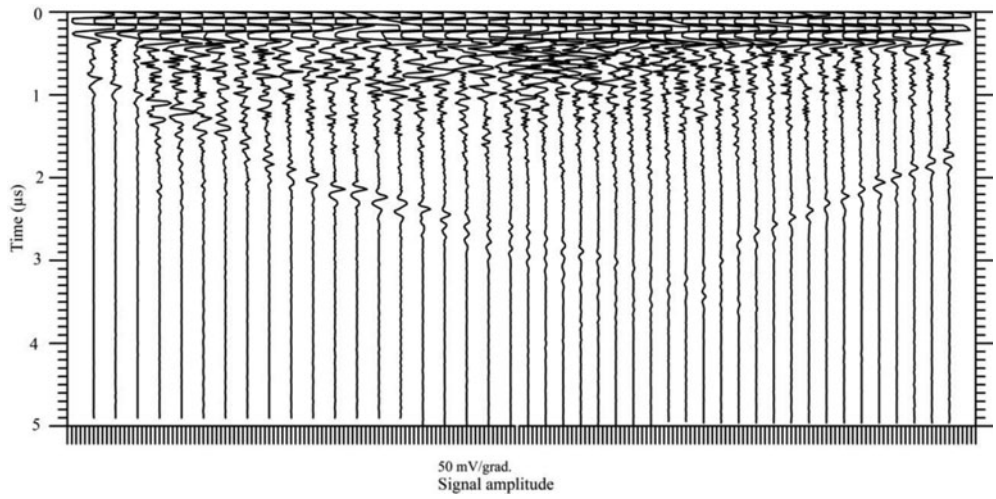

Fig. 4. Radargram of cross section 2: radar signals plotted side by side from west to east in their true spatial relationship to each other (interval between each signal of 10 m). The *x*-axis gives the amplitude of each signal (50 mV per graduation); the *y*-axis is the double-time interval.

https://doi.org/10.3189/2012JoG11J123 Published online by Cambridge University Press

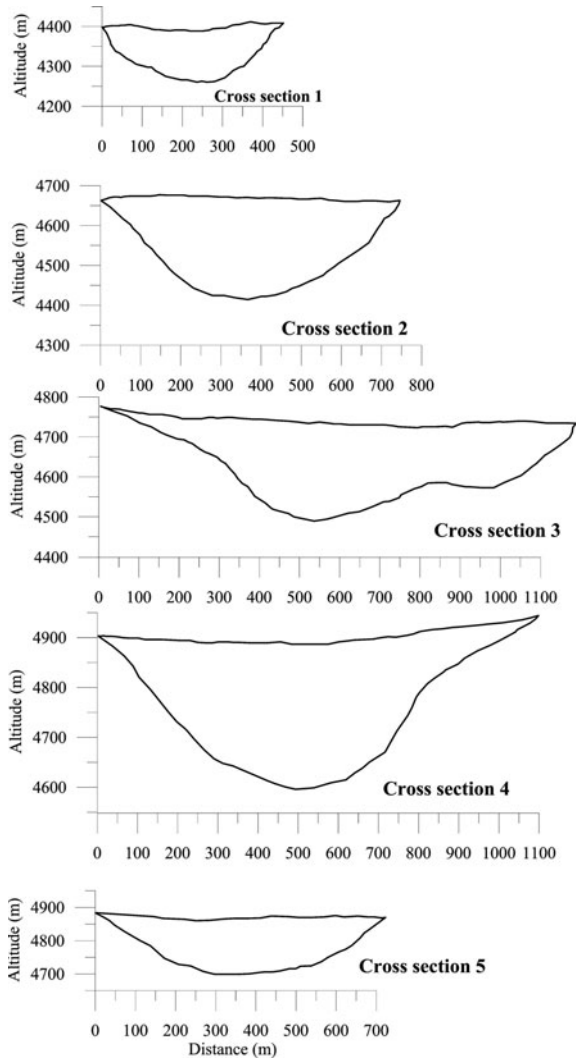

Fig. 5. Ice depth and surface topography of cross sections 1–5. The horizontal and vertical scales are the same for all cross sections. All cross sections are oriented from west to east except cross section 5 which is north–south oriented.

respectively. Reliable velocity measurements could not be made with SPOT5 imagery for other cross sections. Using the mean value of 0.79, the mean horizontal velocity was calculated from the centre-line velocity for each gate cross section (Table 1).

3.4. Ice fluxes from kinematic method

The ice flux Q (m^3 ice a^{-1}) through each cross section was calculated using the cross-sectional area S_c (m^2) and depth-averaged horizontal ice velocity U ($m\,a^{-1}$).

$$Q = US_c \quad (2)$$

The depth-averaged horizontal ice velocity was derived from the mean surface ice velocity calculated in Section 3.3. Nye (1965) gives ratios of depth-averaged horizontal ice velocity to mean surface ice velocity varying from 0.8 (no sliding) to 1 (maximum sliding). Here we assume a mean basal sliding, with a constant ratio of 0.9. The calculated ice fluxes and maximum depth at each cross section are given in Table 1. The flux through cross section 3 at 4750 m a.s.l. is higher than the flux through cross section 4 at 4900 m a.s.l. This is due to the ice influx from the western part of the glacier (flux through cross section 5) which contributes to cross section 3 and not to cross section 4 (Fig. 1).

The largest uncertainty in the depth-averaged horizontal ice velocity results from the ratio between the depth velocity and the surface flow velocity. The estimated factor 0.9 and unknown variations in the basal sliding lead to an uncertainty of roughly ±10% in the calculated flux, which lies within the range of uncertainty of the other variables as discussed by Huss and others (2007). Consequently, we can infer that depth-averaged horizontal ice velocity at each cross section is known with an accuracy of 1.0–3.0 $m\,a^{-1}$ depending on the cross sections. Combining these errors in the cross-sectional area and mean velocity, the uncertainties in the ice fluxes are 0.21, 0.69, 0.92, 0.89 and 0.38×10^6 $m^3\,a^{-1}$ for cross sections 1, 2, 3, 4 and 5 respectively. We have considered the errors to be systematic, so these uncertainties are probably overestimated.

3.5. Ice fluxes obtained from surface mass balance

We also calculated ice fluxes using annual surface mass balance measured during 2002–10. Although dynamic changes are neglected here, this method allows us to estimate the ice fluxes for each section from mass-balance data according to

$$Q = \frac{1}{0.9}\sum_{z}^{z_{max}} b_i s_i \quad (3)$$

where Q is the ice flux (converted into m^3 ice a^{-1} using an ice density of 900 $kg\,m^{-3}$, hence the factor 1/0.9) at a given elevation, z, and b_i is the annual mass balance of the

Table 1. Calculated ice flux, mean surface ice velocity and maximum ice depth at each cross section. The mean surface horizontal ice velocities are from DGPS measurements performed in 2003/04. The satellite-derived mean ice velocities are from the correlation of satellite images acquired on 13 November 2004 and 21 September 2005 (NA: not available)

Cross section	Altitude	Cross-sectional area	Mean surface ice velocity from field data*	Satellite-derived mean surface velocity	Ice flux	Max. depth at centre of cross section
	m a.s.l.	10^4 m^2	$m\,a^{-1}$	$m\,a^{-1}$	10^6 $m^3\,a^{-1}$	m
1	4400	4.23 ± 0.68	20.3	NA	0.78 ± 0.21	124
2	4650	12.14 ± 1.09	31.2	30.7	3.41 ± 0.69	240
3	4750	16.49 ± 1.65	29.2	29.2	4.35 ± 0.92	245
4	4900	15.53 ± 1.55	30.1	NA	4.20 ± 0.89	270
5	4850	6.01 ± 0.90	27.1	25.5	1.47 ± 0.38	175

*Centre-line velocity × 0.79.

https://doi.org/10.3189/2012JoG11J123 Published online by Cambridge University Press

Table 2. Ice fluxes (10^6 m^3 ice a^{-1}), inferred at each cross section from annual mass-balance data

Cross section	Altitude	Hydrological year (Oct–Sep)								Mean (2002–10)
		2002/03	2003/04	2004/05	2005/06	2006/07	2007/08	2008/09	2009/10	
	m a.s.l.									
Snout	4050	–22.26	–19.28	2.27	–22.21	–15.59	–14.65	2.06	5.24	–10.55
1	4400	–22.83	–19.55	3.78	–22.65	–15.43	–14.82	3.19	6.84	–10.18
2	4670	–14.31	–11.49	6.57	–14.35	–8.63	–8.21	6.03	8.70	–4.46
3	4735	–9.88	–7.68	6.89	–10.04	–5.45	–5.46	6.16	8.43	–2.13
4	4900	–1.41	–1.36	4.84	–2.30	0.05	–0.16	4.14	5.72	1.19
5	4870	–1.61	–1.30	2.08	–2.19	–0.57	–0.82	1.86	2.80	0.03

altitudinal range i of map area s_i. The altitudinal ranges taken into account in the calculation are located between z and the highest range of the glacier z_{max} (highest altitude of the glacier area contributing ice to the cross section). We assume that at each point of the glacier above z the surface elevation has remained unchanged from one year to the next.

The ice fluxes calculated from annual mass-balance data at the five cross sections each year are given in Table 2 (further below), while the average ice fluxes for the 8 years are given in Figure 7. The uncertainties in ice fluxes resulting from surface mass balance are directly derived from the mass-balance uncertainties (see Section 3.1) applied to areas contributing to each cross section.

4. DISCUSSION

The first and main objective of this section is to discuss the mass-balance change of Chhota Shigri glacier over the last two to three decades using not only direct glacier-wide mass-balance observations (over the last 8 years) but also ice-flux analysis. The second goal is to give insights into the specific dynamics and the future retreat of this glacier that can be expected in relation to its recent surface mass balance (SMB).

4.1. Null to slightly positive mass balance during the 1990s inferred from ice fluxes

The ice fluxes obtained by the kinematic method using ice thickness and 2003/04 ice velocities are much higher than the average fluxes derived from the 2002–10 SMBs, the latter often being negative (Table 2). Thus, to assess the mean state of the glacier corresponding to the ice fluxes obtained by the kinematic method, here we compare these measured ice fluxes to theoretical ice fluxes calculated from SMB assuming the glacier to be in steady state. The glacier-wide mass balance obtained by the glaciological method is –0.67 m w.e. a^{-1} over the 2002–10 period. Consequently, the SMB needs to be increased by 0.67 m w.e. a^{-1} for the glacier to be in steady state with the present surface area. For each year (2002–10), we calculated the theoretical ice flux from SMB at each cross section assuming the glacier was in steady state. For this purpose, every year, a theoretical SMB at each elevation has been calculated by subtracting the overall annual specific SMB of the same year. For instance, year 2002/03 was characterized by an annual glacier-wide SMB of –1.42 m w.e., so we calculated a new SMB profile by adding 1.42 m w.e. to the SMB at each elevation. In contrast, 2009/10 was characterized by an annual glacier-wide SMB of +0.33 m w.e., so we calculated a new SMB profile by subtracting 0.33 m w.e. from the SMB at each elevation. The

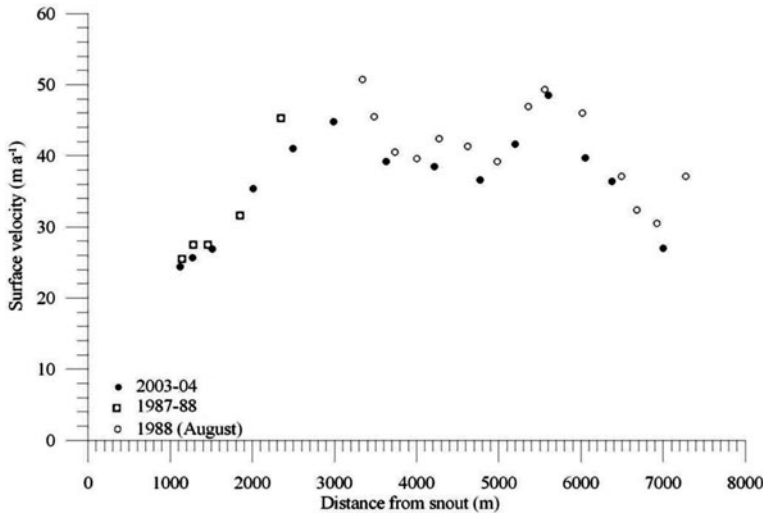

Fig. 6. Measured ice velocities plotted as a function of the distance from the 2010 terminus position. Measurements were collected along the central flowline.

https://doi.org/10.3189/2012JoG11J123 Published online by Cambridge University Press

Table 3. Ice fluxes (10^6 m^3 ice a^{-1}), obtained at every cross section, using steady-state mass-balance assumption for every surveyed year

Cross section	Altitude	Hydrological year (Oct–Sep)								Mean (2002–10)	Std dev.
		2002/03	2003/04	2004/05	2005/06	2006/07	2007/08	2008/09	2009/10		
	m a.s.l.										
Snout	4050	0.00	0.00	0.00	0.00	0.00	0.00	0.00	0.00	0.00	0
1	4400	1.25	1.32	1.33	1.38	1.43	1.03	0.96	1.17	1.23	0.17
2	4670	5.07	5.30	4.59	4.99	4.94	4.55	4.24	4.14	4.73	0.41
3	4735	6.04	6.11	5.27	5.85	5.70	5.02	4.69	4.68	5.42	0.58
4	4900	5.78	4.87	4.11	4.88	5.09	4.58	3.48	4.02	4.60	0.72
5	4870	2.76	2.48	1.63	2.17	2.49	2.06	1.46	1.77	2.10	0.46

resulting ice fluxes are reported in Table 3, together with the mean ice flux at each cross section over the 8 years and the corresponding standard deviations.

These ice fluxes are close to the 2003/04 ice fluxes obtained by the kinematic method (Fig. 7), indicating that the dynamic behaviour of the glacier in 2003/04 is representative for steady-state conditions. This suggests that during the one to two decades preceding 2003/04, the glacier-wide mass balance of this glacier has probably been close to zero and that, in 2003/04, the ice fluxes had not adjusted to the last 3–4 years' negative SMB.

This result is also supported by other observations. First, the ice velocities measured in 1987/88 (Dobhal and others, 1995) are very close to the 2003/04 values (Fig. 6), suggesting that the dynamic behaviour of the glacier did not change much between 1988 and 2004. Second, the terminus fluctuation measured between 1988 and 2010 shows a moderate retreat of 155 m, equivalent to only 7 m a^{-1}, in agreement with conditions not far from steady state. Given that Berthier and others (2007) observed a glacier-wide SMB of Chhota Shigri glacier of approximately –1 m w.e. a^{-1} during the period 1999–2004, the glacier is likely to have experienced a null to slightly positive mass balance between 1988 and the end of the 20th century.

4.2. Glacier dynamics starting to adjust to 21st-century negative SMB

In theory, the response of ice fluxes to surface mass balance is immediate (Cuffey and Paterson, 2010, p. 468), but observations show a 1–5 year delay (Vincent and others, 2000, 2009; Span and Kuhn, 2003). For instance, Span and Kuhn (2003) found synchronous decrease in ice velocity between eight glaciers in the European Alps, which are driven by the same mass-balance changes (Vincent and others, 2005). Consequently, the recent dynamic behaviour of Chhota Shigri glacier should be affected by the negative mass balance since 1999. However, the stake network on Chhota Shigri glacier, originally designed for SMB measurements, is not best suited to accurately compare either the ice velocities or the thickness variations because the measurements have not been performed at exactly the same location every year and are mainly restricted to the ablation area.

In spite of the above limitation, an attempt has been made to compare ice velocities and elevations from the available stake network. For this purpose, stakes measured at the beginning and end of the series have been selected on five short longitudinal cross sections (A–E in Fig. 1) along the centre line of the glacier where the network is most dense. The elevations in 2003 and 2010 and the ice velocities in

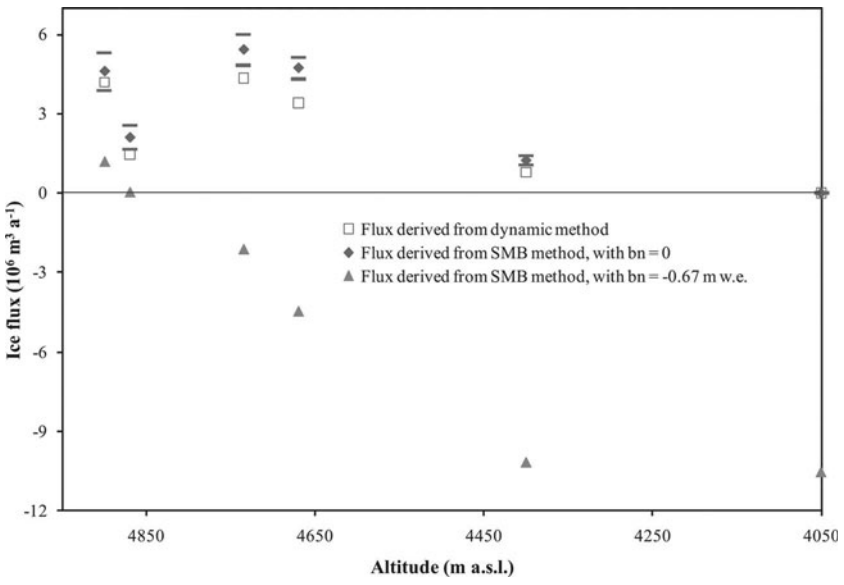

Fig. 7. Ice fluxes at every cross section derived from 2003/04 ice velocities and section areas (open squares), and from mass-balance method for a glacier-wide SMB = 0 m w.e. (plain squares) or a glacier-wide SMB = –0.67 m w.e. (triangles). The error range for mass-balance fluxes calculated from the mass-balance method assuming a steady state (±1 standard deviation: hyphens) is also given.

https://doi.org/10.3189/2012JoG11J123 Published online by Cambridge University Press

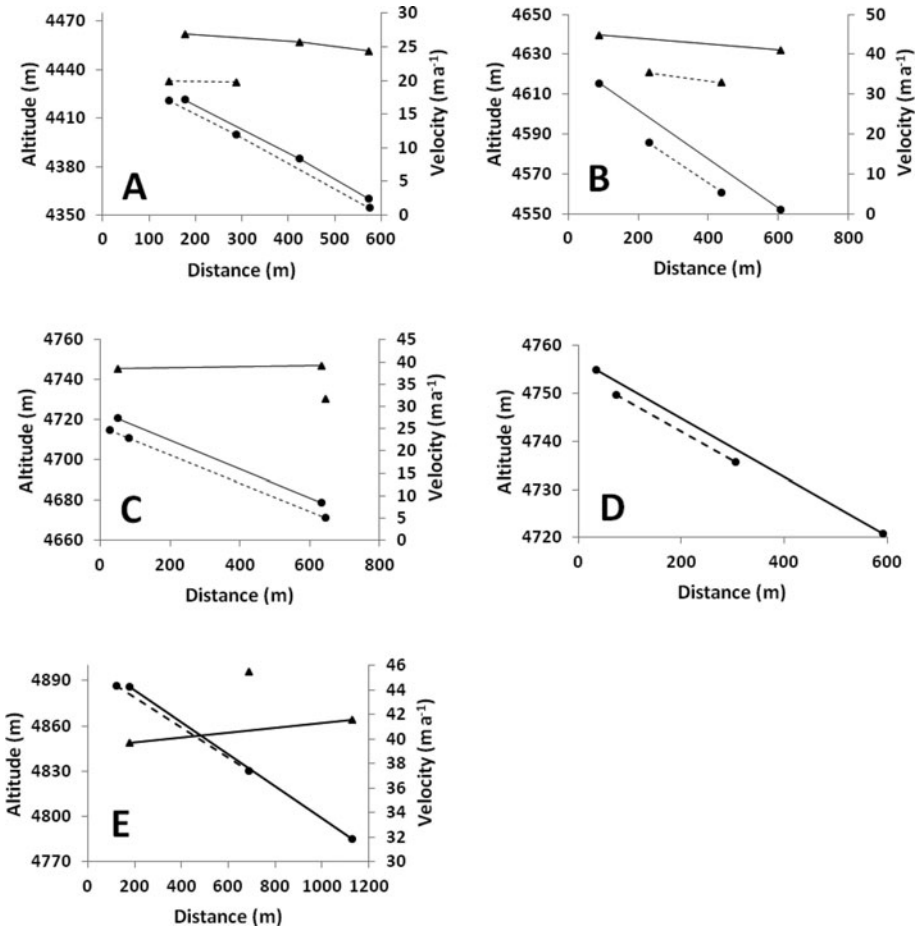

Fig. 8. Elevation (dots) and surface ice velocity (triangles) between 2003 (solid lines) and 2010 (dashed lines) along the longitudinal sections A–E shown in Figure 1.

2003/04 and 2009/10 have been reported on these longitudinal cross sections to deduce thickness and velocity changes in the ablation area (Fig. 8; Table 4). Although the accuracy of the results is affected by the distance between the point measurements, we conclude that the part of the glacier below 4750 m a.s.l. is in strong recession. First, the thickness has decreased by 0.7–1.1 m a^{-1} over the last 7 years. Second, the ice velocities have decreased by ~7 m a^{-1} between 2003 and 2010, resulting in a 24–37% decrease in the ice fluxes since 2003. Despite an improvable monitoring network, it may be surmised that the ice fluxes have been affected by the negative glacier-wide mass balance during (at least) the last 8 years, and the glacier dynamics are progressively adjusting to the negative SMB. Consequently, we expect terminus retreat to accelerate in forthcoming years. If the SMB remained equal to its 2002–10 average value in the future, the terminus would retreat by 5.6 km to reach 4870 m a.s.l. (the altitude where the ice flux is equal to zero) (Table 2).

5. CONCLUSION

Chhota Shigri glacier experienced negative mass balance over the 2002–10 period. The glacier-wide mass balance is estimated at –0.67 m w.e. a^{-1} between 2002 and 2010, revealing strong unsteady-state conditions over this period. Conversely, ice fluxes calculated through five transverse cross sections by the kinematic method correspond to near-steady-state conditions before 2004. Given that ice velocities measured in 2003/04 are close to those measured in 1988, and that the terminus has retreated only 155 m between 1988 and 2010, it seems that the dynamic change was moderate between 1988 and 2004. Therefore, considering that Berthier and others (2007) observed a negative glacier-wide mass balance of about –1 m w.e. a^{-1} between 1999 and 2004 using satellite images, our analysis suggests that the glacier experienced a period of slightly positive or near-zero mass balance at the end of the 20th century, before starting to shrink. As Chhota Shigri seems to be representative of other glaciers in the Pir Panjal range (Berthier and others, 2007), it is possible that many Western Himalayan glaciers of northern India experienced growth during the last 10–12 years of the 20th century, before starting to shrink at the beginning of the 21st century.

Since 2003, ice velocities and elevation in the ablation area have decreased. Our data suggest that the ice fluxes have diminished by 24–37% below 4750 m a.s.l. between 2003 and 2010. Even if we account for a 37% decrease in ice fluxes calculated from 2003/04 ice velocities to obtain present ice flux values, there remains a very large imbalance with ice fluxes from glacier-wide mass balance in the last 8 years. Thus the present dynamics (thickness and ice velocities) of the glacier are far from surface mass-balance and climate conditions of the last 8 years, even if it is progressively adjusting. Therefore the glacier is likely to undergo accelerated retreat in the near future.

Chhota Shigri glacier is almost free of debris, so its mass-balance variations are closely related to climate changes. It

https://doi.org/10.3189/2012JoG11J123 Published online by Cambridge University Press

Table 4. Thickness and surface velocity changes between 2003 and 2010 on five longitudinal cross sections (NA: not available)

Long. section	Elevation change	Velocity change
	m	m a^{-1}
A	–5.3	–6.6
B	–8.6	–8.8
C	–7.5	–7.4
D	–2.8	NA
E	–5.6	+4.8

has the longest-running series of mass-balance measurements in the Himalaya range. More detailed investigations of the dynamic behaviour and the mass balance are needed in the future, although such field measurements are demanding due to the very high altitude. In order to investigate the annual thickness and the ice velocity changes, we recommend performing elevation and ice velocity measurements on ~12 cross sections including some in the accumulation zone. We also recommend measuring the ice velocities from a dense network of stakes to be set up on longitudinal centre lines in order to compare the annual velocity changes at the same points. Finally, we recommend calibrating and checking the mass-balance field measurements from a volumetric method (from photogrammetry or remote-sensing techniques).

ACKNOWLEDGEMENTS

This work has been supported by the IFCPAR/CEFIPRA under project No. 3900-W1 and by the French Service d'Observation GLACIOCLIM as well as the Department of Science and Technology (DST), and Space Application Centre, Government of India. The French National Research Agency through ANR-09-CEP-005-01/PAPRIKA provided DGPS devices to perform field measurements. We thank J.E. Sicart, J.P. Chazarin, our field assistant B.B. Adhikari and the porters who have taken part in successive field trips, sometimes in harsh conditions. We also thank D.P. Dobhal for his kind cooperation in answering our queries regarding earlier research on Chhota Shigri glacier. E. Berthier acknowledges support from the French Space Agency (CNES) through the TOSCA and ISIS proposal No. 0507/786 and from the Programme National de Télédétection Spatiale (PNTS). We thank Jawaharlal Nehru University for providing all the facilities to carry out this work. K.A. Brugger and an anonymous reviewer provided constructive suggestions and comments which helped to significantly improve the manuscript.

REFERENCES

Barnett TP, Adam JC and Lettenmaier DP (2005) Potential impacts of a warming climate on water availability in snow-dominated regions. *Nature,* **438**(7066), 303–309 (doi: 10.1038/nature04141)

Berthier E and 7 others (2005) Surface motion of mountain glaciers derived from satellite optical imagery. *Remote Sens. Environ.,* **95**(1), 14–28

Berthier E, Arnaud Y, Kumar R, Ahmad S, Wagnon P and Chevallier P (2007) Remote sensing estimates of glacier mass balances in the Himachal Pradesh (Western Himalaya, India). *Remote Sens. Environ.,* **108**(3), 327–338

Bhambri R, Bolch T, Chaujar RK and Kulshreshtha SC (2011) Glacier changes in the Garwal Himalaya, India, from 1968 to 2006 based on remote sensing. *J. Glaciol.,* **57**(203), 543–556 (doi: 10.3189/002214311796905604)

Bookhagen B and Burbank DW (2006) Topography, relief, and TRMM-derived rainfall variations along the Himalaya. *Geophys. Res. Lett.,* **33**(8), L08405 (doi: 10.1029/2006GL026037)

Cogley JG (2009) Geodetic and direct mass-balance measurements: comparison and joint analysis. *Ann. Glaciol.,* **50**(50), 96–100

Cogley JG, Kargel JS, Kaser G and Van der Veen CJ (2010) Tracking the source of glacier misinformation. *Science,* **327**(5965), 522

Cuffey KM and Paterson WSB. (2010) *The physics of glaciers*, 4th edn. Butterworth-Heinemann, Oxford

Dobhal DP, Kumar S and Mundepi AK (1995) Morphology and glacier dynamics studies in monsoon–arid transition zone: an example from Chhota Shigri glacier, Himachal Himalaya, India. *Current Sci.,* **68**(9), 936–944

Dobhal DP, Gergan JT and Thayyen RJ (2008) Mass balance studies of the Dokriani Glacier from 1992 to 2000, Garhwal Himalaya, India. *Bull. Glacier Res.,* **25**, 9–17

Dyurgerov MB and Meier MF (2005) *Glaciers and the changing Earth system: a 2004 snapshot.* Institute of Arctic and Alpine Research, University of Colorado, Boulder, CO (INSTAAR Occasional Paper 58)

Gardelle J, Arnaud Y and Berthier E (2011) Contrasted evolution of glacial lakes along the Hindu Kush Himalaya mountain range between 1990 and 2009. *Global Planet. Change,* **75**(1–2), 47–55 (doi: 10.1016/j.gloplacha.2010.10.003)

Hubbard B and Glasser N. (2005) *Field techniques in glaciology and glacial geomorphology.* Wiley, New York

Huss M, Sugiyama S, Bauder A and Funk M (2007) Retreat scenarios of Unteraargletscher, Switzerland, using a combined ice-flow mass-balance model. *Arct. Antarct. Alp. Res.,* **39**(3), 422–431

Huss M, Bauder A and Funk M (2009) Homogenization of long-term mass-balance time series. *Ann. Glaciol.,* **50**(50), 198–206 (doi: 10.3189/172756409787769627)

Kulkarni AV (1992) Mass balance of Himalayan glaciers using AAR and ELA methods. *J. Glaciol.,* **38**(128), 101–104

Kulkarni AV and 6 others (2007) Glacial retreat in Himalaya using Indian remote sensing satellite data. *Current Sci.,* **92**(1), 69–74

Kumar S (1999) Chhota Shigri glacier: its kinematic effects over the valley environment, in the northwest Himalaya. *Current Sci.,* **77**(4), 594–598

Machguth H, Eisen O, Paul F and Hoelzle M (2006) Strong spatial variability of snow accumulation observed with helicopter-borne GPR on two adjacent Alpine glaciers. *Geophys. Res. Lett.,* **33**(13), L13503 (doi: 10.1029/2006GL026576)

Mattson LE, Gardner JS and Young GJ (1993) Ablation on debris covered glaciers: an example from the Rakhiot Glacier, Punjab, Himalaya. *IAHS Publ.* 218 (Symposium at Kathmandu 1992 – *Snow and Glacier Hydrology*), 289–296

Narod BB and Clarke GKC (1994) Miniature high-power impulse transmitter for radio-echo sounding. *J. Glaciol.,* **40**(134), 190–194

Nijampurkar VN and Rao DK (1992) Accumulation and flow rates of ice on Chhota Shigri glacier, central Himalaya, using radioactive and stable isotopes. *J. Glaciol.,* **38**(128), 43–50

Nye JF (1965) The flow of a glacier in a channel of rectangular, elliptic or parabolic cross-section. *J. Glaciol.,* **5**(41), 661–690

Oerlemans J (2001) *Glaciers and climate change.* A.A. Balkema, Lisse

Ohmura A, Bauder A, Müller H and Kappenberger G (2007) Long-term change of mass balance and the role of radiation. *Ann. Glaciol.,* **46**, 367–374 (doi: 10.3189/172756407782871297)

Paterson WSB (1994) *The physics of glaciers*, 3rd edn. Elsevier, Oxford

Raina VK, Kaul MK and Singh S (1977) Mass-balance studies of Gara Glacier. *J. Glaciol.,* **18**(80), 415–423

Roy SS and Balling RC, Jr (2005) Analysis of trends in maximum and minimum temperature, diurnal temperature range, and cloud

cover over India. *Geophys. Res. Lett.,* **32**(12), L12702 (doi: 10.1029/2004GL022201)
Singh P, Jain SK and Kumar N (1997) Estimation of snow and glacier-melt contribution to the Chenab River, western Himalaya. *Mt. Res. Dev.,* **17**(1), 49–56
Solomon S and 7 others eds. (2007) *Climate change 2007: the physical science basis. Contribution of Working Group I to the Fourth Assessment Report of the Intergovernmental Panel on Climate Change*. Cambridge University Press, Cambridge
Span N and Kuhn M (2003) Simulating annual glacier flow with a linear reservoir model. *J. Geophys. Res.,* **108**(D10), 4313 (doi: 10.1029/2002JD002828)
Thibert E, Blanc R, Vincent C and Eckert N (2008) Glaciological and volumetric mass-balance measurements: error analysis over 51 years for Glacier de Sarennes, French Alps. *J. Glaciol.,* **54**(186), 522–532 (doi: 10.3189/002214308785837093)
Vincent C (2002) Influence of climate change over the 20th century on four French glacier mass balances. *J. Geophys. Res.,* **107**(D19), 4375 (doi: 10.1029/2001JD000832)
Vincent C, Vallon M, Reynaud L and Le Meur E (2000) Dynamic behaviour analysis of glacier de Saint-Sorlin, France, from 40 years of observations, 1957–97. *J. Glaciol.,* **46**(154), 499–506 (doi: 10.3189/172756500781833052)
Vincent C, Kappenberger G, Valla F, Bauder A, Funk M and Le Meur E (2004) Ice ablation as evidence of climate change in the Alps over the 20th century. *J. Geophys. Res.,* **109**(D10), D10104 (doi: 10.1029/2003JD003857)
Vincent C, Le Meur E, Six D and Funk M (2005) Solving the paradox of the end of the Little Ice Age in the Alps. *Geophys. Res. Lett.,* **32**(9), L09706 (doi: 10.1029/2005GL022552)
Vincent C, Soruco A, Six D and Le Meur E (2009) Glacier thickening and decay analysis from 50 years of glaciological observations performed on Glacier d'Argentière, Mont Blanc area, France. *Ann. Glaciol.,* **50**(50), 73–79 (doi: 10.3189/172756409787769500)
Wagnon P and 10 others (2007) Four years of mass balance on Chhota Shigri Glacier, Himachal Pradesh, India, a new benchmark glacier in the western Himalaya. *J. Glaciol.,* **53**(183), 603–611
Yadav RR, Park W-K, Singh J and Dubey B (2004) Do the western Himalayas defy global warming? *Geophys. Res. Lett.,* **31**(17), L17201 (doi: 10.1029/2004GL020201)
Zemp M, Hoelzle M and Haeberli W (2009) Six decades of glacier mass-balance observations: a review of the worldwide monitoring network. *Ann. Glaciol.,* **50**(50), 101–111 (doi: 10.3189/172756409787769591)

MS received 23 June 2011 and accepted in revised form 3 December 2011